Relationships between Antarctic cyclones and surface conditions as derived from high-resolution numerical weather prediction data

P. Uotila,[1] T. Vihma,[2] A. B. Pezza,[3] I. Simmonds,[3] K. Keay,[3] and A. H. Lynch[4]

Received 18 November 2010; accepted 27 January 2011; published 14 April 2011.

[1] An Antarctic cyclone climatology was created based on simulations of the Antarctic Mesoscale Prediction System (AMPS) and the University of Melbourne Cyclone (UM) detection and tracking algorithm for the period 2001–2009. Over 17,000 cyclone tracks were included in the climatology, and 20% of these cyclones were mesoscale in terms of their size. Mesoscale systems were common south of the Antarctic Circumpolar Trough (ACT) over the coastal oceans of the Indian Ocean sector and in the Ross Sea, while large synoptic systems occurred most frequently in the ACT. A novel technique was applied to study the relationships between cyclone characteristics and surface properties over the Southern Ocean and the coastal areas of Antarctica. Our comprehensive study has revealed that up to half of the cyclones simulated by AMPS correlated with the surface latent heat flux, sensible heat flux, or temperature gradient. These cyclones either modified the surface or were being modified by it. In the former category, 85% of the systems were synoptic cyclones associated predominantly with baroclinicity and advection, and the atmospheric boundary layer had a little influence in the generation and development of cyclones. On the contrary, in the latter category, 36% of the systems were mesoscale cyclones gaining energy from instabilities in the boundary layer associated with strong turbulent fluxes.

Citation: Uotila, P., T. Vihma, A. B. Pezza, I. Simmonds, K. Keay, and A. H. Lynch (2011), Relationships between Antarctic cyclones and surface conditions as derived from high-resolution numerical weather prediction data, *J. Geophys. Res.*, *116*, D07109, doi:10.1029/2010JD015358.

1. Introduction

[2] The atmospheric circulation of the Southern Hemisphere and the associated poleward flow of heat and moisture originating from lower latitudes strongly influence the state and evolution of the Antarctic Ice Sheet [*Peixoto and Oort*, 1992]. Along with its surrounding sea ice, Antarctica plays a major part in the radiative forcing of high southern latitudes, with links back to the atmospheric and oceanic circulation [*Mo*, 2000; *Rasmussen and Turner*, 2003; *Arbetter et al.*, 2004; *Wassermann et al.*, 2006; *Delworth and Zeng*, 2008; *Pezza et al.*, 2008; *Turner et al.*, 2009a; *Udagawa et al.*, 2009]. For example, the continental ice sheet reduces Southern Hemisphere temperatures and strongly influences the cyclone tracks around the continent [*Walsh et al.*, 2000; *Simmonds and Keay*, 2000]. The amount and variability of the poleward atmospheric moisture transport has been quantified by studies on the Antarctic moisture convergence [*Bromwich et al.*, 1995; *Cullather et al.*, 1998; *Zou et al.*, 2004; *Tietäväinen and Vihma*, 2008], and low-pressure systems form a very important part of this transport [*King and Turner*, 1997; *Simmonds and Keay*, 2000; *Noone and Simmonds*, 2002]. Other studies have found direct links between Antarctic atmospheric temperature and precipitation anomalies and circulation patterns over the Southern Ocean [*Genthon et al.*, 2003; *Lynch et al.*, 2006; *Uotila et al.*, 2007; *Krinner et al.*, 2007; *Monaghan et al.*, 2008] acting over a range of time scales. Because transient low-pressure systems have a central role in the atmospheric circulation of the Southern Hemisphere, the understanding of their generation, evolution and decay is required in order to obtain a comprehension of Southern Hemisphere climate. Additionally, these low-pressure systems significantly impact the local weather and their accurate forecasting is important for aviation and field safety. Several studies have addressed the behavior and nature of synoptic systems [*Simmonds and Keay*, 2000; *Simmonds et al.*, 2003; *Hodges et al.*, 2003; *Pezza and Ambrizzi*, 2003; *Hoskins and Hodges*, 2005; *Wang et al.*, 2006; *Bromwich et al.*, 2007; *Yuan et al.*, 2009; *Turner et al.*, 2009b; *Ulbrich et al.*, 2009; *Uotila et al.*, 2009] based on operational analysis and reanalysis data sets and their fundamental importance for the Antarctic weather and climate is currently understood relatively well [*Turner and Pendlebury*, 2004]. A ring of low-pressure systems is

[1]CSIRO Marine and Atmospheric Research, Aspendale, Victoria, Australia.
[2]Finnish Meteorological Institute, Helsinki, Finland.
[3]School of Earth Sciences, University of Melbourne, Melbourne, Victoria, Australia.
[4]School of Geography and Environmental Science, Monash University, Melbourne, Victoria, Australia.

0148-0227/11/2010JD015358

located in the Antarctic Circumpolar Trough (ACT) from 50°S to 70°S [*King and Turner*, 1997]. This region affects many aspects of the Antarctic climate. Synoptic systems move from the ACT southward and when reaching the Antarctic coast, they usually turn to the east moving parallel to the steep continental ice sheet. The ACT and regions south of it are regions of actively decaying cyclones [*Simmonds and Keay*, 2000].

[3] We have less understanding of the nature and characteristics of smaller and short-lived mesoscale cyclones, which often go undetected between weather stations, are difficult to detect from satellite images and require high-resolution numerical models to be simulated. For example, *Condron et al.* [2006] estimated that only around 40% of cyclones having radii of 250 km were detected from the ERA-40 reanalysis data. As a consequence their role in the meridional moisture transport remains poorly quantified. Additionally, mesoscale systems can have gale-force winds and pose a risk for human activities in the region. Many observational studies have addressed their occurrence [*Carleton and Carpenter*, 1990; *Carleton and Fitch*, 1993; *Carrasco et al.*, 2003], dynamics [*Heinemann*, 1990; *Bromwich*, 1991; *Carrasco and Bromwich*, 1993; *Turner et al.*, 1993a; *Fantini and Buzzi*, 1993] and their role in relation to the climate system [*Carleton and Carpenter*, 1990; *Lubin et al.*, 2008; *Yuan et al.*, 2009] since the beginning of the satellite era. The formation of polar mesoscale cyclones is often related to synoptic conditions and the cold air advection due to enhanced katabatic winds [*Carrasco and Bromwich*, 1993] with subsequent growth sustained by the air-sea interaction [*Fitch and Carleton*, 1991] over relatively warm ocean. It is possible that the mesoscale systems are more frequent just outside the sea ice zone than previously thought [*Irving et al.*, 2010] and their occurrence is closely related to synoptic conditions and the heterogeneous surface.

[4] New extensive studies have recently been published, as data have become available, focusing on the occurrence of mesoscale cyclones [*Claud et al.*, 2009a, 2009b; *Yuan et al.*, 2009; *Patoux et al.*, 2009; *Irving et al.*, 2010], but only limited sets of surface related interactions have been considered. The spatial gradients across the ice-ocean interface cause significant baroclinic instability, which impacts on the cyclonic activity over the south Southern Ocean [*Simmonds and Budd*, 1991; *Simmonds and Wu*, 1993; *Raphael*, 2003]. The quantitative importance of different surface related factors and their association to cyclone characteristics has not been estimated so far by using comprehensive data. *Simmonds et al.* [2005] estimated large-scale fluxes of momentum and mechanical energy in the Antarctic sea ice region based on a relatively coarse resolution NCEP-DOE reanalysis. They found that cyclonic activity contributes at least 60% to these fluxes over the sea ice and the ocean to the north. Additionally, *Watkins and Simmonds* [1995] found that sea ice concentration induces anomalies in the atmospheric parameters in time scales of less than 5 days in numerical weather prediction (NWP) runs. Accordingly, the use of a realistic distribution of sea ice concentration produces results distinct from forecasts obtained with an unchanging sea ice concentration distribution. *Saetra et al.* [2008] observed that strong wind forcing from polar lows can lead to surface warming due to the entrainment of subsurface warm water in the Nordic Seas and believed that this could be a positive feedback mechanism for cyclone intensity. However, a model study by *van Lipzig and van den Broeke* [2002] suggests that the atmospheric boundary layer over the sea ice region responds passively to the large-scale circulation rather than being a driving force for the meridional moisture transport. The impact of surface properties on the meridional transport of heat and moisture is likely to be apparent on longer interannual time scales as demonstrated by model simulations, where reduced winter sea ice in the Southern Hemisphere led to warmer temperatures and increased precipitation farther south [*Noone and Simmonds*, 2004].

[5] Here, for the first time, a large number of cyclones and associated surface conditions based on high-resolution data are harvested and multivariate statistics are generated. A synthesis of relationships between cyclone properties and underlying surface conditions is quantified covering a wider range of circumstances than has been considered heretofore. This enables a comprehensive characterization of the interplay between cyclones and sea ice in the Antarctic, which has not yet been clearly understood. It will be shown that deep synoptic cyclones modify the ocean surface, the sea ice cover and turbulent heat fluxes. On the contrary, weaker mesoscale cyclones are shown to be generated and impacted by the surface temperature gradients and turbulent heat fluxes.

2. Data and Methods

2.1. The Antarctic Mesoscale Prediction System

[6] The Antarctic Mesoscale Prediction System (AMPS) has provided operational weather forecasts for the Antarctic region since September 2000 [*Powers et al.*, 2003]. These forecasts provide essential guidance for logistical and scientific operations in Antarctica and surrounding oceans where the weather station network is sparse. The system uses WRFVAR 3D Variational data assimilation to assimilate available observations. The AMPS system has undergone several changes during its functioning period (Table 1) and has output available from the 5th of January 2001 to the present, with a 3 h interval. The atmospheric model employed was the Polar Mesoscale Model 5 (Polar-MM5) [*Bromwich et al.*, 2001; *Cassano et al.*, 2001] until March 2006, when the polar-optimized version of the Weather Research and Forecasting model (Polar-WRF) was implemented [*Skamarock et al.*, 2005, 2008; *Hines and Bromwich*, 2008]. The modifications to the AMPS system configuration, such as changes in the computational grid and physical parameters, affect both the performance of the model and the temporal integrity of the record. This has to be borne in mind when analyzing the output data and one has to be careful not to derive conclusions of the atmospheric variability based on these artifacts. For details of the AMPS system configuration see the AMPS website at http://www.mmm.ucar.edu/rt/amps/ and *Bromwich et al.* [2005].

[7] AMPS produces forecasts for up to 120 h and is initialized twice daily at 0000 and 1200 UTC. For this study, the forecast hours of 3–12 were selected since they are available more than 97% of the time. If data from these forecast hours were missing hours 15–24 were selected from the data archive. The performance of AMPS has been evaluated by *Guo et al.* [2003] and *Bromwich et al.* [2005], who found it to produce skillful forecasts, and hence performance will not be evaluated further here.

Table 1. Annual Numbers of Cyclones

Year	Number of Cyclones			Notes[a]
	All	Large	Small	
2001	1535	1341	194	Horizontal resolution set to 90 km.
2002	1724	1462	262	The model domain was extended as shown in Figure 1.
2003	1960	1657	303	
2004	1986	1665	321	
2005	1941	1594	347	
2006	1865	1489	376	Data start in March as the atmospheric model changed from Polar MM5 to WRF and resolution increased to 60 km.
2007	2418	1845	573	
2008	2352	1707	645	Resolution increased to 45 km.
2009	1411	1034	377	Data end in July.
Total	17192	13794	3398	

[a]Notes describe major changes in the AMPS configuration.

[8] In this study, the AMPS data are utilized to study the weather patterns and the occurrence of mesoscale cyclones over the Southern Ocean and Antarctica. Although the available AMPS data cover a relatively short period for a climatological study (January 2001 to July 2009) they have a higher resolution both spatially and temporally compared to the usually used global model analyses and reanalyses. *Trenberth and Fasullo* [2010] found that reanalyses and global coupled climate models show the largest biases of absorbed solar radiation over the Antarctic sea ice region, where also the cyclonic activity between AMPS and three reanalyses products differs most [*Uotila et al.*, 2009]. Few studies have focused on the performance of AMPS at the mesoscale. *Bromwich et al.* [2003] found that AMPS was able in a case study to predict a mesoscale low, although not at the observed locations. AMPS also showed skill in simulating upper-level conditions realistically and in resolving features with a small vertical scale, such as katabatic winds. *Steinhoff et al.* [2008] found that AMPS underestimated the wind speed during a storm at McMurdo station, Antarctica, due to a misplacement of a hydraulic jump downstream of downslope windstorms. *Seefeldt and Cassano* [2008] analyzed low-level jets across the Ross Ice Shelf region based on 5 years of AMPS data, and *Parish et al.* [2006] assessed the mean structure of the Ross Ice Shelf air stream, and both studies found good agreement with observations. *Schlosser et al.* [2008] studied the precipitation regime of Dronning Maud Land by using 6 years of data from the AMPS archive. The AMPS precipitation regime showed a good qualitative agreement with precipitation observations. These studies demonstrate that AMPS can realistically simulate many meteorological processes of the Antarctic atmosphere. Additionally, the above-mentioned studies have shown that polar processes are better represented in the AMPS output than in reanalyses due to the polar specific parameterizations and optimizations of AMPS. These include higher resolution and with it a better representation of complex topography, the inversion layer, katabatic flow and interaction with sea ice.

2.2. Cyclone Detection Algorithm

[9] Cyclone detection and tracking from AMPS data were carried out by using the University of Melbourne Automatic Cyclone Tracking Scheme [*Murray and Simmonds*, 1991a, 1991b; *Simmonds et al.*, 1999; *Simmonds and Murray*, 1999; *Lim and Simmonds*, 2002; *Simmonds*, 2003; *Simmonds et al.*, 2003; *Lim and Simmonds*, 2007] (the UM tracking scheme). The results presented here are based on the tracking analysis using the optimal instruction parameter values as derived by *Uotila et al.* [2009].

[10] A low-pressure system can be characterized by a set of variables, which can be divided to four groups, as follows.

[11] 1. A set of variables provided by the UM tracking scheme includes system time, system location (longitude, latitude), intensity (I [hPa (°lat)$^{-2}$]), radius (R [°lat]), depth (D [hPa]) and central pressure among others and they contain one point value per system location. The intensity is calculated as the Laplacian of the pressure field in the vicinity at the center of the system. The system depth is calculated directly by the UM tracking scheme as described by *Simmonds and Keay* [2000], and depends on the system intensity and radius. For example, for the idealized case of an axially symmetric paraboloidal depression the system depth is calculated as

$$D = {}^1/_4 I\, R^2. \quad (1)$$

[12] 2. Based on the UM tracking scheme output, a set of variables summarizing the characteristics of cyclones can be computed. These variables include lifetime, track length, mean speed, maximum radius and genesis location and time among others. Variables of this kind were used to derive subsets of systems. For example, a set of small systems was indentified using the constraint of a maximum radius smaller than 4.5 degrees of latitude. In theory the smallest system radius that can be identified for a given resolution data set is the grid resolution (45 km for the AMPS data). The Melbourne University cyclone tracking scheme smoothes input data horizontally and applies a relatively complex algorithm when determining the radius of a system. Hence the systems with R close to the theoretical minimum are not detected by the scheme, and the minimum radius for systems detected from the AMPS output was 1.2 degrees of latitude.

[13] 3. Variables related to system properties can be derived from the AMPS archive. These variables include precipitation (P), downward shortwave radiation (SWR_d), downward longwave radiation (LWR_d), and variables derived from wind velocity, such as speed (WS) and convergence (C). WS and C were calculated at 10 m or, if missing, at the lowest vertical model level horizontal wind components. These variables are described by a number of grid point values. Here the set was defined by the system size as the set of grid points inside the circle within the system radius R from its center location. All convective fluxes were defined to be positive upward and negative downward.

[14] 4. Variables related to surface properties can be derived from the AMPS archive. These variables include sea surface temperature (SST) and its gradient ($\partial_s SST$), surface temperature (T_s) and its gradient ($\partial_s T_s = [\max(T_s) - \min(T_s)]/R$), sensible and latent heat fluxes (H and LE) and sea ice concentration IC. Over the open ocean $T_s = SST$ while in partially ice covered grid cells SST is the average surface temperature of the open water and T_s the average temperature of the entire grid cell. Temperature gradients

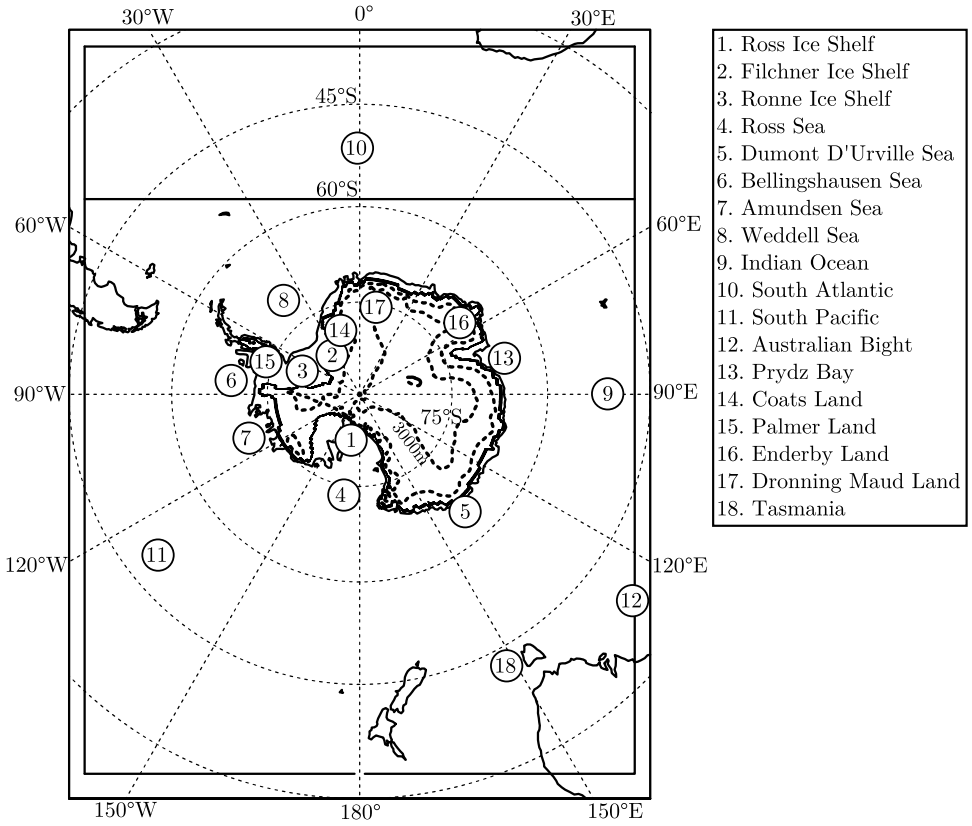

Figure 1. A map covering the largest AMPS domain marked with a rectangle extending from Australia to South Africa. Major geographic locations are marked with circled numbers. Thick dashed lines represent surface elevation of the Antarctic Ice Sheet with isolines every 1000 m. A horizontal line north of 60°S in the South Atlantic marks the boundary of the largest AMPS domain before July 2002.

were estimated based on T_s, because under cold conditions and on ice or snow surfaces $\partial_s SST$ is not necessarily large, as *SST* cannot go below the freezing point, although T_s gradient can be. *IC* was provided by the National Snow and Ice Data Center [*Comiso*, 1999] from 2001 to 2007 and from 2008 onward *IC* was derived from the AMPS archive.

2.3. Cyclone Database

[15] The UM tracking algorithm detected a large number of systems that occurred close to steep topographical features over land and moved with velocities that were unrealistic for a low-pressure system. Additionally many systems entered or left the model domain and their characteristics over their lifetime, such as the conditions of formation or decay, remain unknown. Systems selected for this study were constrained to those that were generated and decayed within the model domain, had a lifetime longer than 12 h and did not travel across terrain higher than 500 m except when the distance between their first and last locations was more than 1000 km. When these criteria were applied, the systems that behaved unrealistically close to steep topographic features were excluded. After this filtering 17,192 tracks were detected by the UM tracking scheme (Table 1), comprising 326,105 3-hourly cyclone locations for the analysis indicating that the average lifetime for these systems is approximately 2 days and 9 h.

[16] In this study, we explore the behavior of mesoscale cyclones as distinct from their synoptic-scale counterparts. To do this we must obtain a physically based and objective method of specifying the scale separation. The validity of the quasi-geostrophic (synoptic) approximation can be tested by using two conditions associated with the ageostrophic components of the motion [*Gill*, 1982; *Vallis*, 2006]: (1) the isallobaric effect needs to be small $T \gg f^{-1}$, and (2) the acceleration is small compared to the Coriolis and pressure gradient forces $Ro = U/(f_o L) \ll 1$. Here L is the characteristic length scale, T is the characteristic time scale and U is the characteristic speed. f_0 is the Coriolis parameter and Ro is the Rossby number. If the motion does not satisfy these conditions it has nonsynoptic, i.e., mesoscale, characteristics. By assuming a latitude range from 40°S to 80°S, the first condition gives $T \gg 2$ h, and the second one $U/L \ll 10^{-4}$ s^{-1} for the quasi-geostrophic approximation to be valid. This means that systems with relatively short characteristic time scales, $T < 2$ days, are probably not synoptic systems. It is a reasonable conclusion that these systems have short lifetimes. Additionally, systems that remain small, $L < 1000$ km, and move fast, $U \sim 10$ m/s, are probably not synoptic. Accordingly, systems having a radius up to 500 km can be considered as mesoscale systems with a high probability. This limit also represents a convenient and commonly applied approximation to the upper limit of mesoscale activity [*Irving et al.*, 2010].

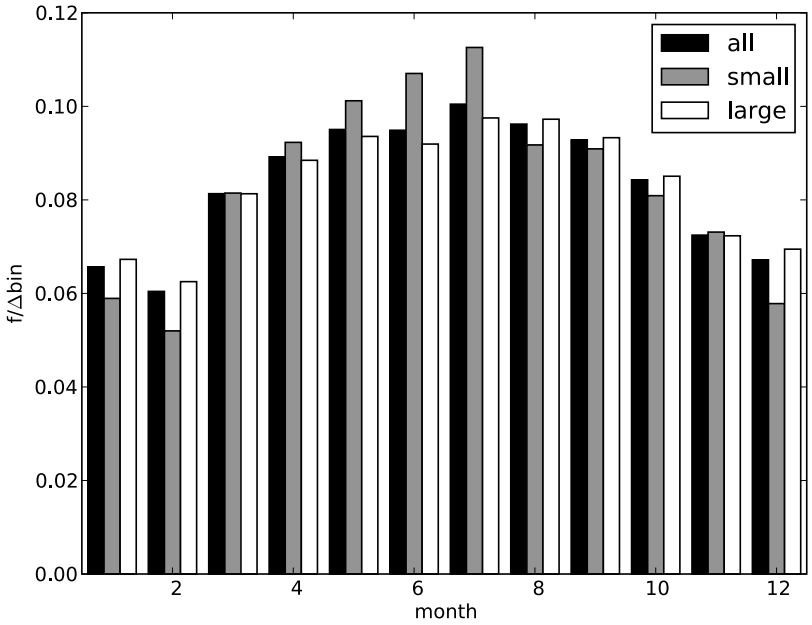

Figure 2. Monthly frequencies of system genesis with distribution of all detected systems is plotted as black bars, distribution of small systems subset is plotted as gray bars, and distribution of large systems subset is plotted as white bars. Each distribution is presented as a density function so that its integral is equal to 1.

[17] Following the reasoning presented above, a "small systems" subset is derived from detected systems with a requirement that the system maximum radius during its life is less than 500 km. This subset contains 3398 systems, which is about 20% of all systems. The "small systems" average lifetime is short, less than 28 h. The "large systems" subset is the complement of the "small systems" subset having an average lifetime of 2 days and 16 h. Accordingly a minority but significant proportion of systems generated inside the AMPS domain are short-lived mesoscale systems.

3. Results

3.1. Variability of Cyclone Activity

3.1.1. Temporal Variability

[18] The number of systems detected by the tracking scheme increases from 2001 to 2009 (Table 1). This mostly reflects the changes in the AMPS system configuration, namely in the resolution, and various refinements including domain size (Figure 1 and Table 1). During the first 2 years of its operation the number of systems remained small when compared to years 2003–2009. From 2001 to July 2002 the largest model domain was smaller than the later period and systems were detected from a smaller area. The ratio between the number of small systems and the number of all systems increased when the atmospheric model was changed from Polar-MM5 to Polar-WRF and the domain resolution increased from 90 km to 60 km in 2006. From 2005 to 2008 the number of systems increased 21%, with a dramatic increase in the number of small systems of 86%. This clearly demonstrates the importance of model resolution when simulating mesoscale systems. The number of large systems, importantly, did not change significantly.

[19] The monthly number of systems is high in winter and low in summer (Figure 2). February is the minimum for cyclonicity in the model domain. The monthly number of systems increases from February to July, when it reaches the maximum. Between April and July the number of small systems is relatively high compared to the number of large systems. It is apparent that although the interannual variability is strongly impacted by the changes in the AMPS model, the seasonal variability is less affected.

3.1.2. Geographical Variability

[20] The geographical distribution of track density of large systems is presented in Figure 3a. The high track density area curves around Antarctica forming about 60°S, which is consistent with earlier studies [e.g., *Simmonds and Keay*, 2000]. The number of large systems drops gradually when approaching the Antarctic continent especially close to the coast of East Antarctica, where few synoptic systems move across the coastal waters of Antarctica toward the continental ice sheet. In summer the ACT contains more large systems over the Amundsen-Bellingshausen Sea and north of the west Weddell Sea than in winter (Figure 3b), while there are more large systems in winter than in summer elsewhere, especially in the Ross Sea and Dumont D'Urville Sea. As a result the ACT in AMPS oscillates seasonally following a semiannual pattern [*Simmonds et al.*, 1998; *Simmonds and Jones*, 1998; *van den Broeke*, 1998].

[21] Small systems do not form as concentrated a track density pattern as the large systems (Figure 4a). Their track densities are relatively low in the ACT, and highest south of the ACT over the coastal oceans of the Indian Ocean sector and in the Ross Sea. They approximately follow the climatological September sea ice edge, either slightly to the north of it (the Dumont D'Urville Sea) or slightly to the south (the Ross Sea and the Indian Ocean sector). In the Ross Sea a large

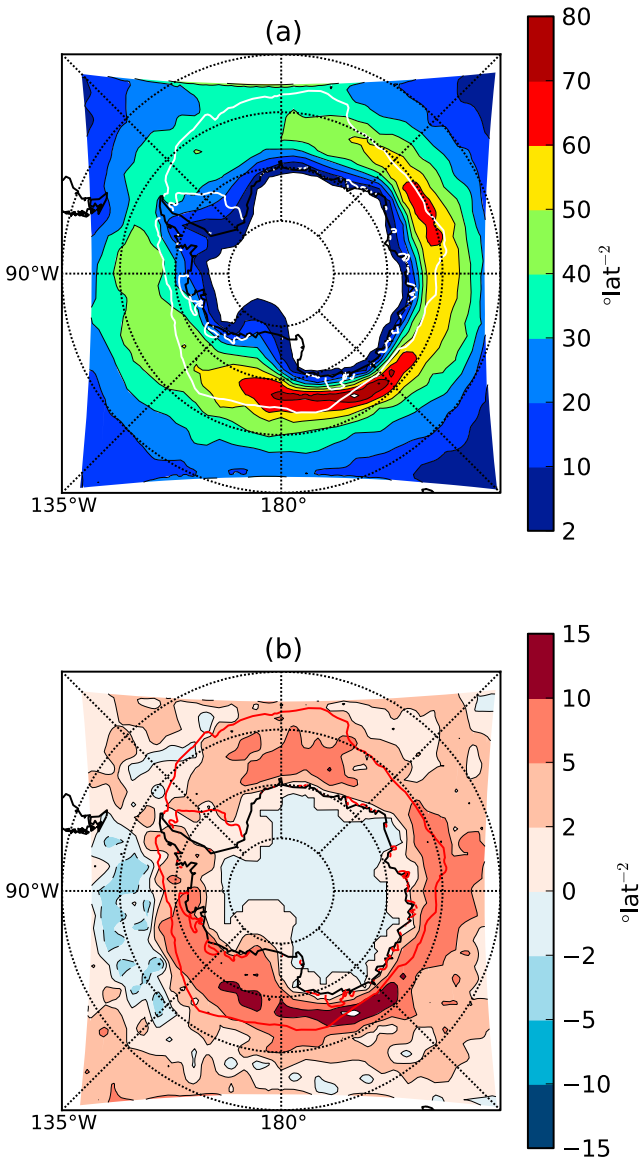

Figure 3. Track densities (the number of tracks per °latitude^2) of (a) cyclones with maximum radius larger than 4.5 °latitude and (b) their difference between winter and summer (JJA–DJF). Continuous lines mark the isolines of 70% mean ice concentration for 2001–2007 in February (inner line) and in September (outer line) around Antarctica.

number of small systems are generated in front of the September climatological sea ice edge over the ocean in winter (Figure 4b) and these are known to be related to cold air outbreaks [*Carleton and Carpenter*, 1990; *Parish et al.*, 2006; *Turner et al.*, 2009b]. There are also more small systems over large parts of the sea ice covered areas in winter than in summer. On the contrary, track densities are slightly higher in the north of the west Weddell Sea in summer than in winter on the lee side of South America. Interestingly, the number of small systems is slightly larger in summer than in winter across a region in the south Weddell Sea just off the summer sea ice edge west of Coats Land. This region is known for its mesoscale cyclone activity in a baroclinic zone separating warm poleward advecting air and cold continental air [*Turner et al.*, 1993b]. In addition, it is possible that some convective systems develop due to large fluxes of heat and moisture over the open water [*Turner and Row*, 1989].

3.2. Relationships Between Cyclone and Surface Variables

3.2.1. Relationships Between Variables Defining Cyclone Characteristics

[22] A set of two-dimensional distributions is illustrated in Figure 5 describing probabilities of the occurrence of

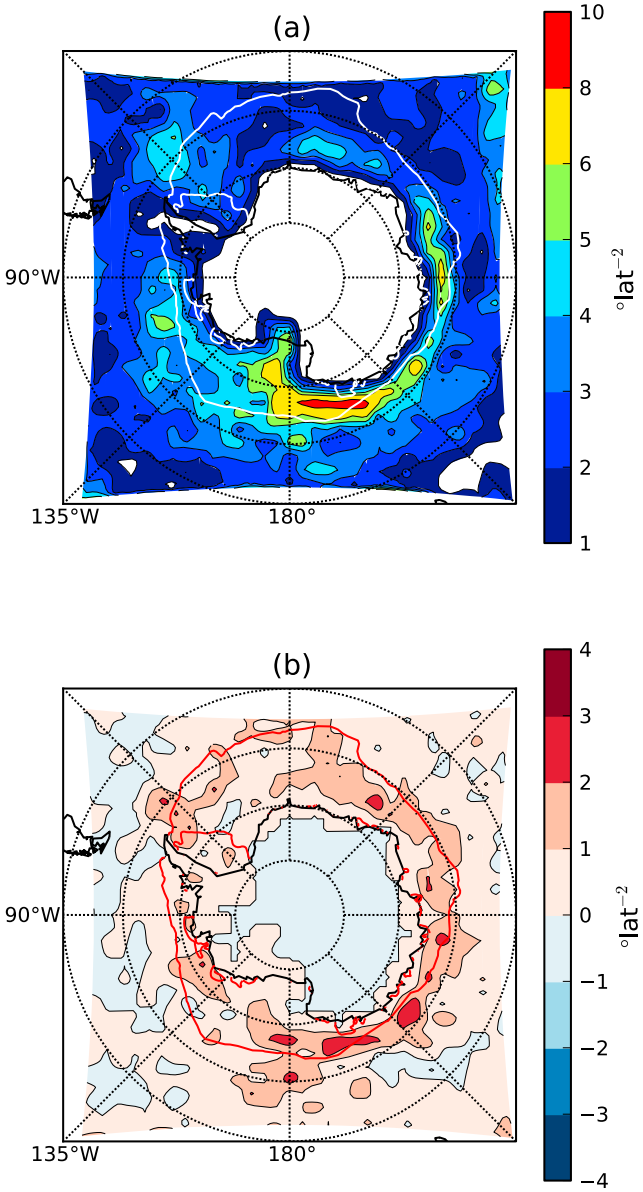

Figure 4. Track densities of (a) cyclones with maximum radius smaller than 4.5 °latitude and (b) their difference between winter and summer (JJA–DJF). Continuous lines mark the isolines of 70% mean ice concentration for 2001–2007 in February (inner line) and in September (outer line) around Antarctica.

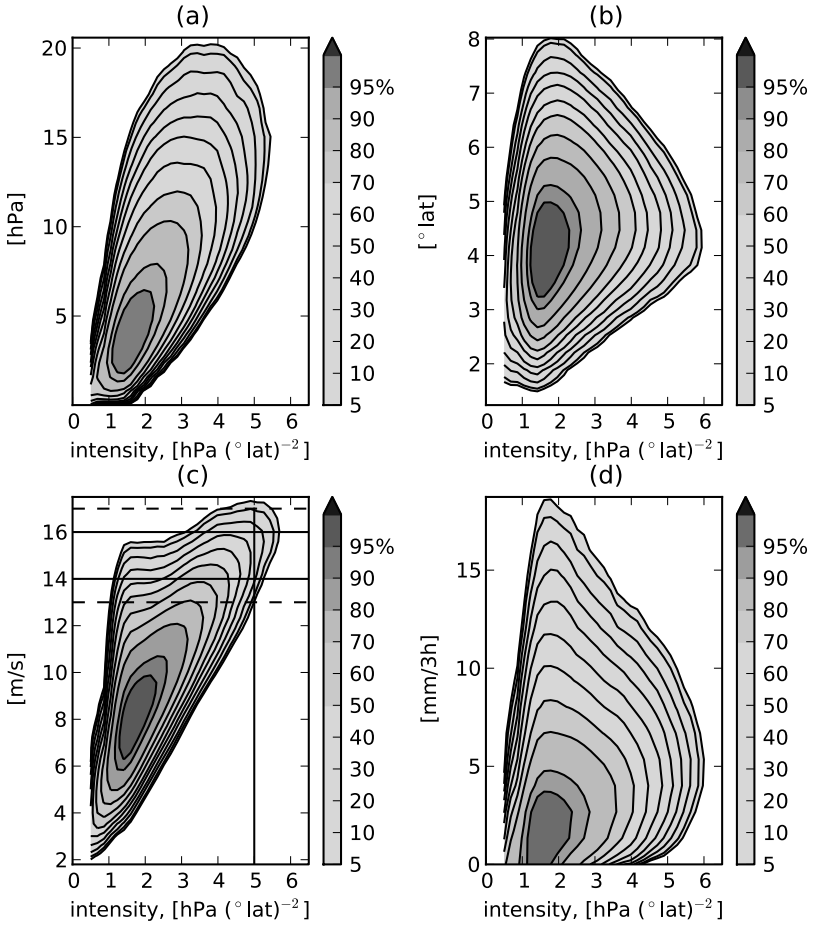

Figure 5. Two dimensional probability distributions between the system intensity (horizontal axis) and (a) system depth, (b) system radius, (c) wind speed, and (d) precipitation. Vertical scale indicates cumulative sums of number of systems as 5, 10, …, 90, and 95% percentile values.

Antarctic cyclones. Distributions of these kinds can be used to identify extreme cyclones and also systems which are not realistic. For example one might want to ascertain how the wind speed varies with very intense systems having $I > 5$ hPa(°lat)$^{-2}$ (vertical line in Figure 5c). Based on system count contours, representing the percentile values of probability distribution, a mean wind speed of almost 16 m/s can be expected (horizontal line), where the values exceeding the range (dashed horizontal lines) represent extreme wind speeds for very intense systems.

[23] Variables characterizing cyclones are mutually dependent, as can be expected from equation (1) and illustrated in Figure 5. Cyclones simulated by AMPS, as shown in Figure 5a, indicate that D increases approximately linearly with I. It is noteworthy that D is directly proportional to the square root of the total kinetic energy of a system [*Simmonds and Keay*, 2009].

[24] Very small systems, having $R < 3$°lat, tend to be less intense than larger systems as shown in Figure 5b, but very large systems, with $R > 6$°lat, are typically not very intense. The most intense systems simulated by AMPS typically have a radius of 4–5°lat, but the variability of I in this size category is very large. The correlation between WS and I is high (Figure 5c): low-intensity systems have low wind speeds and high-intensity systems have high wind speeds. This is because WS is proportional to the pressure gradient and I to the Laplacian of pressure. There are, however, low-intensity systems with strong winds, which have been termed "Merry-Go-Round" systems [*Fitch and Carleton*, 1991; *Rasmussen and Turner*, 2003]. These systems tend to occur adjacent to a relatively strong background flow of the main storm track or are embedded inside high-intensity, high-wind cyclones.

[25] Low-pressure systems with high intensity are associated with high convergence values, while the convergence is smaller with systems of low intensity. Systems that precipitate little are also low in intensity, but, on the other hand, the most intense systems do not have the highest precipitation rates (Figure 5d). Systems bringing the largest amounts of precipitation are large frontal systems with large radii, but relatively low intensities.

3.2.2. Relationships Between Cyclone Characteristics and Surface Properties

[26] Physical relationships explaining how the surface properties impact on cyclone characteristics or vice versa were synthesized by deriving information from a large number of cyclones. Cyclones whose properties significantly correlated with surface characteristics in time were assumed to either modify the underlying surface or to be impacted by it. In the former case cyclone property time

Table 2. Numbers of All Systems and Small Systems in Different Cyclone Categories[a]

Category	Number of Systems		Ratio (%)
	All	Small	
$D \rightarrow H$	1380	192	14
$D \rightarrow \partial_S T_s$	1047	178	17
$D \rightarrow H$ and $D \rightarrow \partial_S T_s$	131	18	14
$H \rightarrow D$	901	197	22
$\partial_S T_s \rightarrow D$	775	200	26
$H \rightarrow D$ and $\partial_S T_s \rightarrow D$	66	21	32

[a] $D \rightarrow H$ ($D \rightarrow \partial_S T_s$) is a system category where system depth impacts on sensible heat (surface temperature gradient) and $H \rightarrow D$ ($\partial_S T_s \rightarrow D$) is a system category where sensible heat (surface temperature gradient) impacts on system depth.

series were assumed to lead surface characteristics time series (in our case by three hours, which is the time resolution of the archived AMPS output), and in the latter case cyclone property time series were assumed to lag surface characteristics time series (by 3 h). Causal relationships are notated as $A \rightarrow B$ when A impacts on B.

[27] System depth was chosen to represent the fundamental cyclone descriptors, because it is intimately related to system radius and intensity, and it correlates significantly with meteorological variables characterizing cyclones as discussed in section 3.2.1. Furthermore, D is proportional to the kinetic energy of system. A large proportion of cyclones correlated with the surface properties: D correlated significantly with H (LE) in 31% (36%) of cyclones, while 19% of cyclones correlated with $\partial_s T_s$ in terms of D. About half (47%) of cyclones did not correlate with any of the surface related variables. Many cyclones had statistically significant causal relationships with surface properties, shown as significant lagged correlations, and 8% (6%) of cyclones modified H ($\partial_s T_s$), and 5% (5%) of cyclones were significantly impacted by H ($\partial_s T_s$). It is plausible to assume that the development and generation of more cyclones were causally associated with the surface conditions than detected, but these causalities could not be identified due to the limited temporal resolution of data.

[28] The numbers of mesoscale systems in cyclone categories depend whether cyclones alter the surface or vice versa (Table 2). When cyclones modify the surface sensible heat flux, latent heat flux and/or temperature gradient, the number of mesoscale cyclones is much smaller (12–17%) than when the sensible heat flux and/or temperature gradient impact on cyclones (22–36%). The largest portion of mesoscale cyclones (36%) is in the category where the sensible and latent heat fluxes and temperature gradient impact on the generation and development of cyclones.

[29] Cyclones in different categories differ significantly in terms of their seasonal occurrence (Figure 6). Cyclones in the category $D \rightarrow H$ occur more frequently than the ones in $D \rightarrow \partial_s T_s$ especially in summer (Figure 6). Numbers of these cyclones don't change much between seasons, because they modify H, mainly via WS. The number of cyclones modifying $\partial_s T_s$ is smaller in summer, when the sea ice is absent,

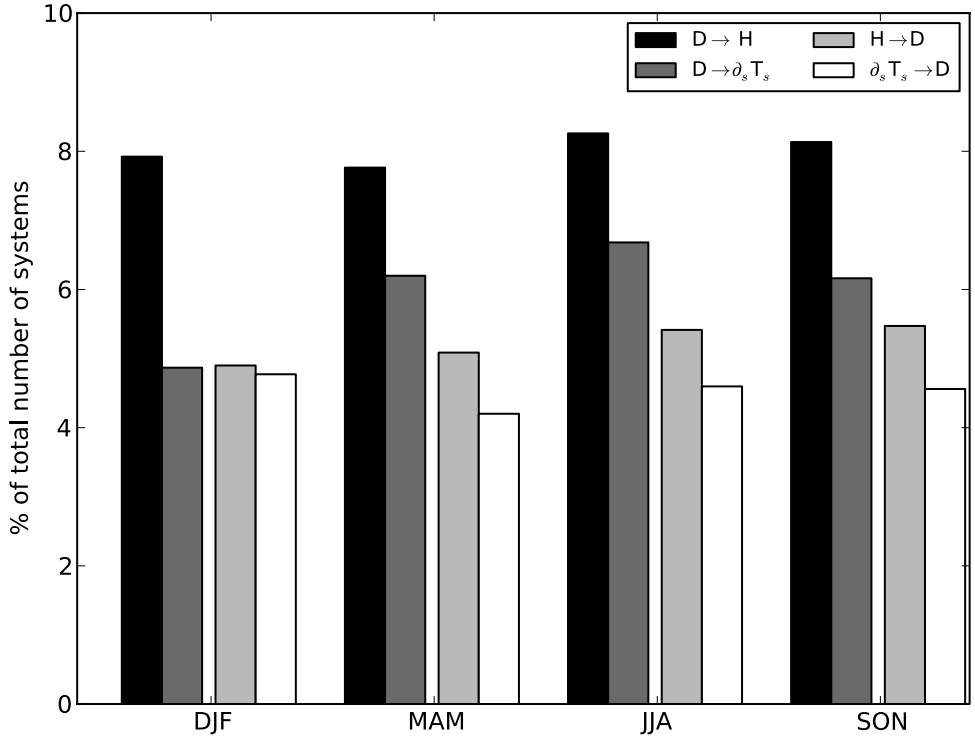

Figure 6. Seasonal distributions of number of systems whose depths correlate with the surface temperature gradient or sensible heat flux at the 95% confidence level. $D \rightarrow \partial_S T_s$ indicates a category where system depth impacts on temperature gradient, $D \rightarrow H$ indicates a category where D impacts on surface sensible heat, $\partial_S T_s \rightarrow D$ indicates a category where $\partial_S T_s$ impacts on D, and $H \rightarrow D$ indicates a category where H impacts on D. Numbers are percentages of total number of systems.

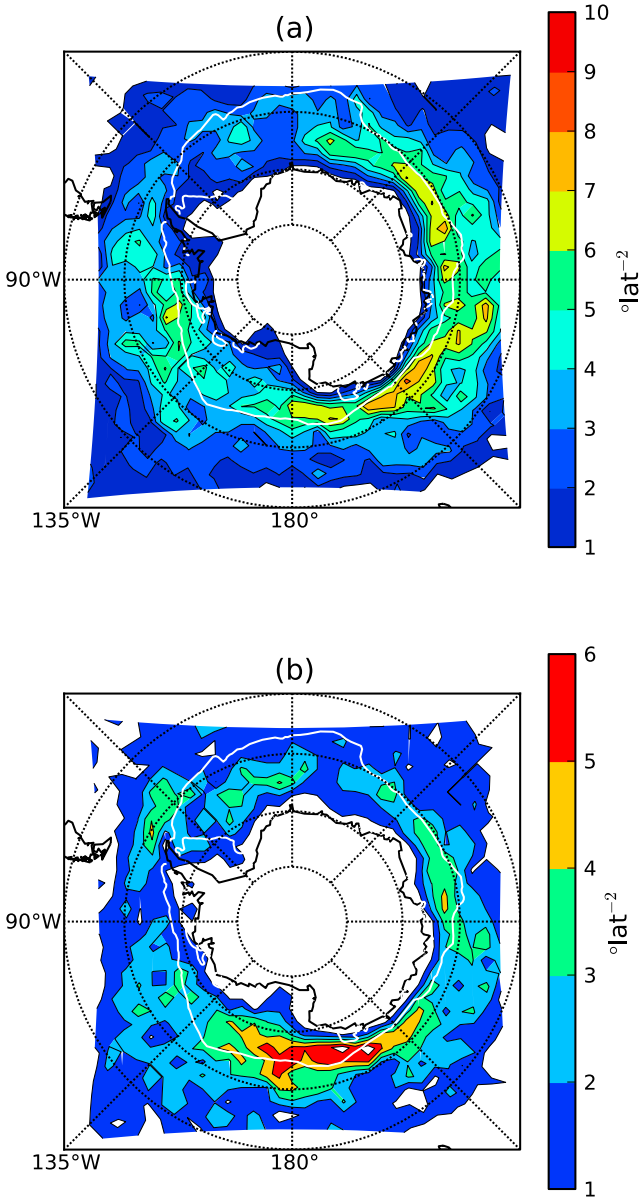

Figure 7. Track densities of systems whose depths correlate with the surface temperature gradient at the 95% confidence level. (a) system depth precedes the temperature gradient and (b) temperature gradient precedes system depth in time. Thick continuous lines mark the isolines of 70% mean ice concentration for 2001–2007 in February (inner line) and in September (outer line) around Antarctica.

than in winter when these cyclones open leads in the sea ice cover and increase $\partial_s T_s$.

[30] Cyclones in two remaining cyclone categories ($H \rightarrow D$ and $\partial_s T_s \rightarrow D$) have quite different seasonal evolution than cyclones in $D \rightarrow H$ and $D \rightarrow \partial_s T_s$. Although their numbers in summer are almost the same, cyclones in $H \rightarrow D$ occur more frequently during other seasons than cyclones in $\partial_s T_s \rightarrow D$. As the temperature difference between the air and ocean becomes larger in winter than in summer, H increases and more heat is released to atmosphere generating and modifying cyclones. The seasonal cycle of $\partial_s T_s \rightarrow D$ behaves in a different way and in summer, large $\partial_s T_s$s are associated with ocean SST fronts, being active regions of cyclonicity, while in winter large $\partial_s T_s$s occur mainly over snow and ice covered surfaces. As a result the number of cyclones in $\partial_s T_s \rightarrow D$ category is largest in summer.

[31] Geographical distributions of cyclones that modify $\partial_s T_s$ (Figure 7a) or H (Figure 8a) resemble the geographical distribution of large cyclones (Figure 3a). This is because deep cyclones, with large radii and intensities, are energetic enough to modify surface properties. On the contrary, the geographical distributions of cyclones that are modified by

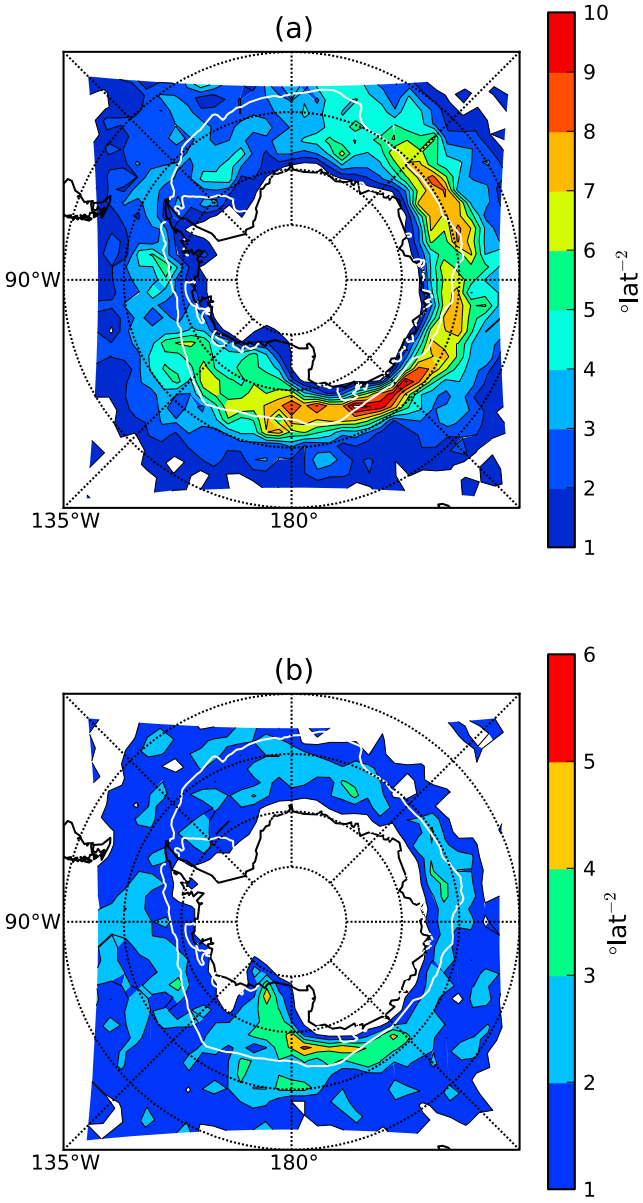

Figure 8. Track densities of systems whose depths correlate with the surface sensible heat at the 95% confidence level. (a) System depth precedes sensible heat and (b) sensible heat precedes system depth in time. Thick continuous lines mark the isolines of 70% mean ice concentration for 2001–2007 in February (inner line) and in September (outer line) around Antarctica.

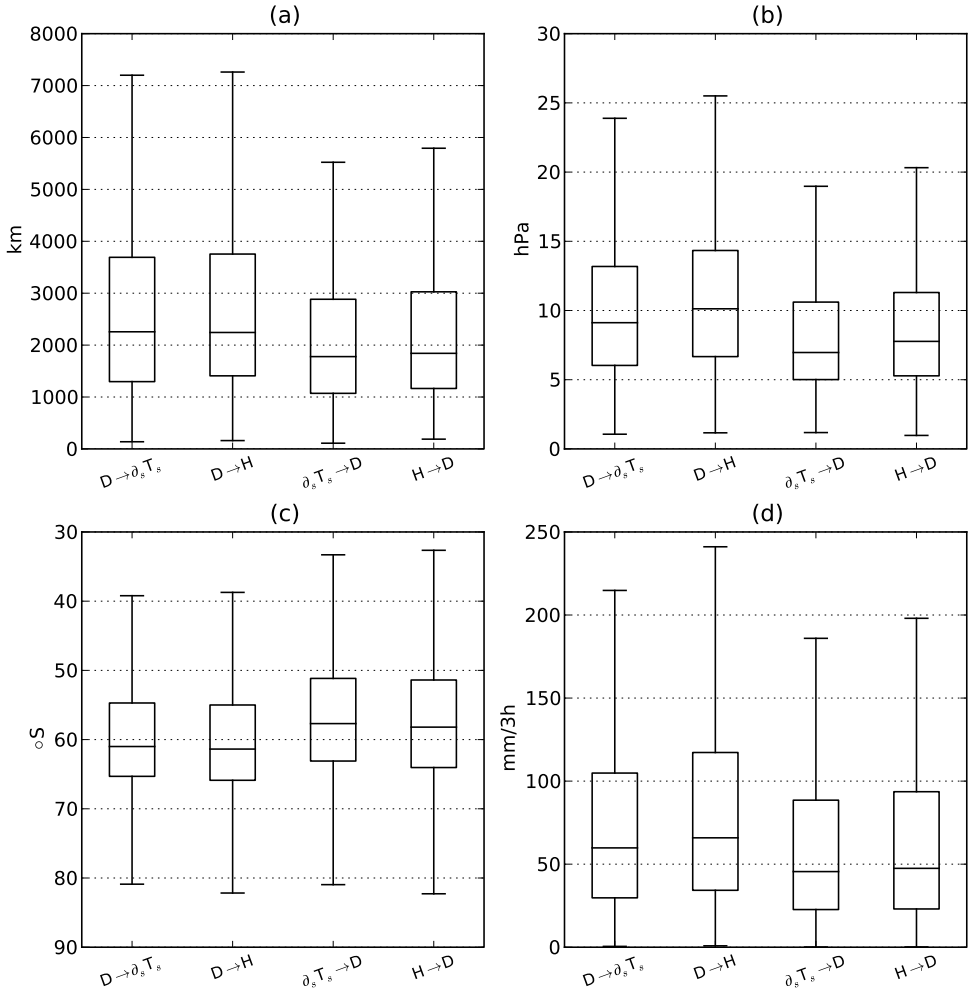

Figure 9. Box plots of systems whose depths correlate with the surface sensible heat or temperature gradient at the 95% confidence level. (a) Track length, (b) system depth, (c) cyclolysis latitude, and (d) system precipitation. Boxes from left to right in each panel represent system categories as in Figure 6. Boxes extend from the lower to upper quartile values of the data, with a line at the median. Whiskers extend from 25% to 75% of data.

$\partial_s T_s$ or H look very different (Figures 7b and 8b) coinciding with regions of high concentrations of mesoscale cyclones (Figure 4a). These cyclones occur mainly over the Ross and Dumont D'Urville Seas. Additionally, $H \rightarrow D$ cyclones occur frequently over the Ross Ice Shelf (Figure 8b), while $\partial_s T_s \rightarrow D$ more common over the open ocean. The generation and development of these mesoscale cyclones are impacted by the surface properties.

[32] Statistics of cyclone properties in different categories show apparent differences closely resembling differences between synoptic cyclones and mesoscale cyclones. Cyclones in categories $D \rightarrow H$ and $D \rightarrow \partial_s T_s$ are likely to have longer track lengths and lifetimes than cyclones in categories $H \rightarrow D$ and $\partial_s T_s \rightarrow D$ (Figure 9a). The average lifetime of cyclones in $H \rightarrow D$ category is 52 h compared to 62 h for cyclones in $D \rightarrow H$ category. Additionally, $D \rightarrow H$ and $D \rightarrow \partial_s T_s$ cyclones are on the average deeper, decay at more southern latitudes and precipitate more than $H \rightarrow D$ and $\partial_s T_s \rightarrow D$ cyclones (Figures 9b–9d). Accordingly synoptic systems transport moisture longer distances and farther south than mesoscale cyclones which tend to develop over the marginal sea ice zone.

[33] It can be expected that the forcing of sea ice distribution by atmospheric stresses is a more dominant factor than anomalous sea ice conditions altering the cyclone motion [*Godfred-Spenning and Simmonds*, 1996], which is shown in this study as a larger number of cyclones impacting the surface than vice versa (Table 2). The impact of cyclones on sea ice concentration can be explored further. Figure 10a shows the relationship between changes in *IC* versus *C*. In cyclones, where *C* is high and wind converges, *IC* is likely to vary a lot and tends to increase on the average. When *C* decreases, *IC* varies less and tends to decrease slightly. Because the Antarctic sea ice drift is mainly divergent, this is to be expected under a weak wind forcing [*Uotila et al.*, 2000]. During powerful storms and highly convergent wind conditions, sea ice is accumulated and *IC* is likely to increase. It is physically consistent to assume that *IC* varies most when it is relatively low, but the internal ice stress resists the *IC* increase when *IC* is high. Hence when *C*

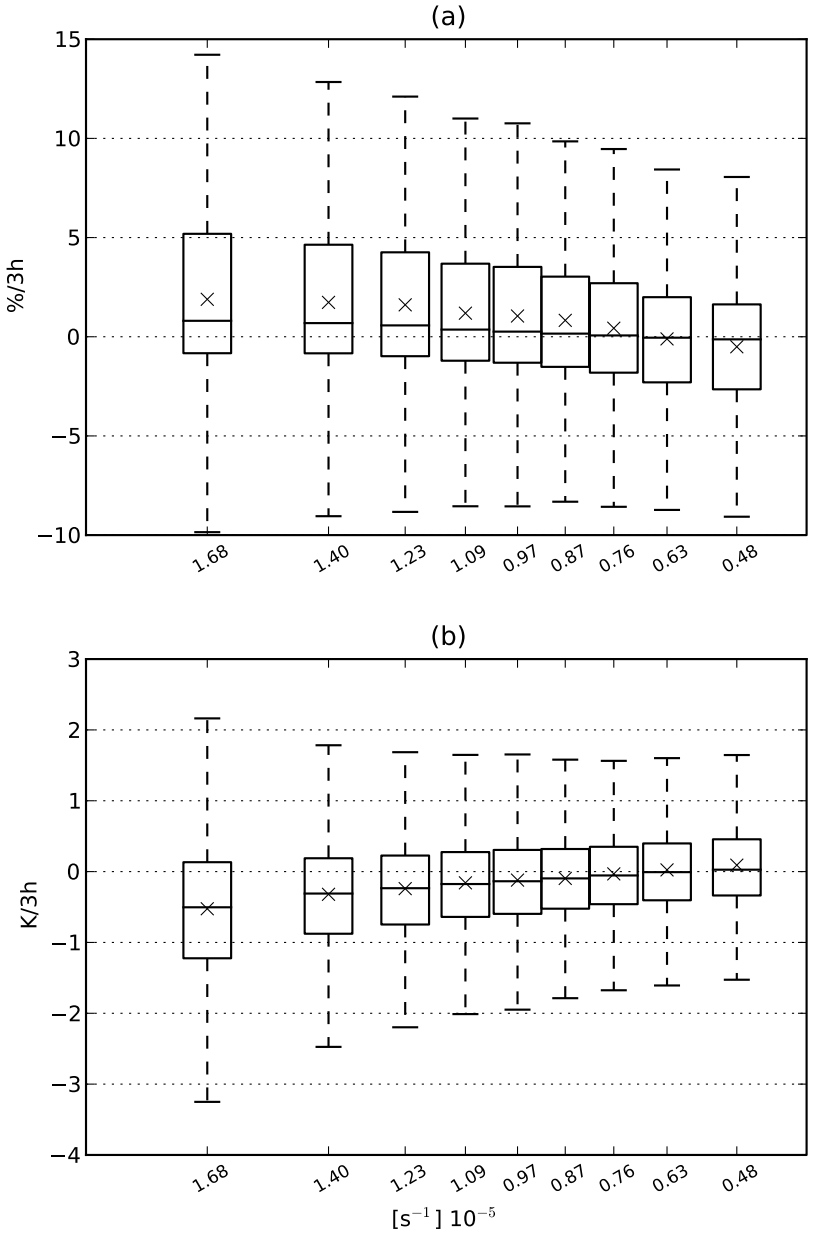

Figure 10. Temporal changes in (a) sea ice concentration and (b) surface temperature versus wind convergence (horizontal axis). Selected systems were generated south of 55°S and located over the partially ice covered ocean. Boxes present data divided by 10, 20, …, 90% percentile values of wind convergence and extend from the lower to upper quartile values of the data, with a line at the median. Whiskers extend from 25% to 75% of data and means are marked with crosses.

is high and *IC* increases significantly, large areas of open water are quickly covered by sea ice. As a result, convergent wind fields modify T_s as well (Figure 10b).

3.2.3. Multivariate Regression Analysis

[34] A multivariate linear regression analysis was performed in order to assess the surface boundary conditions that statistically control *D*. The analysis was carried out separately for each season (DJF, MAM, JJA, SON), when the interseasonal variability is excluded, and for the whole year. The following factors were included as explaining *D*: T_s, $R\partial_S T_s$, *LE*, *H* and *IC*. The surface temperature gradient $\partial_S T_s$ was multiplied by the cyclone radius *R* to eliminate the correlation between *D* and $\partial_S T_s$ due to *R*.

[35] The analyses were made separately for the groups of cyclones listed in Table 2. Results based on cyclones for which $H \rightarrow D$ and $\partial_S T_s \rightarrow D$ and $LE \rightarrow D$ are presented in Table 3. Cyclone depth in this cyclone category was controlled by a combination of several variables with significant seasonal differences and correlations, ranging from 0.08 to 0.40, being high in winter and in summer. RMSE errors reflect the average magnitude of *D*, which is high in winter but small in summer. Annually, in autumn, and in winter T_s and *IC* were the most important variables explaining *D*: cyclones became weaker with increasing T_s and *IC*. These dependencies reflect the fact that cyclones tend to intensify as they approach the Antarctic, as T_s decreases, but then

Table 3. Seasonal Variability of Surface Properties Explaining the Cyclone Depth D by Assuming a Linear Dependence[a]

Period	Surface Properties	r^2	RMSE
Annual	$D = f(-T_s, -IC, +R\partial_S T_s)$	0.22	4.2
Summer	$D = f(+R\partial_S T_s, +LE)$	0.37	1.3
Spring	$D = f(+LE)$	0.08	2.5
Winter	$D = f(-T_s, -IC, +LE)$	0.40	5.9
Autumn	$D = f(-T_s, -IC, +R\partial_S T_s, +H)$	0.25	2.4

[a]Cyclones were selected from the group where $H \rightarrow D$ and $\partial_S T_s \rightarrow D$ and $LE \rightarrow D$. Surface properties are listed in the order of importance from left to right. RMSE denotes the root mean square error and r^2 the correlation between the values predicted by the linear model and observations.

they weaken as they move over areas of increasing sea ice cover and/or the continental ice sheet, as IC approaches unity. The surface temperature variability, $R\partial_S T_s$, increases with D indicating that strong surface temperature gradients increase the kinetic energy of cyclones. The turbulent fluxes of latent and sensible heat contribute toward deeper cyclones in all four seasons, but do not increase r^2 for the annual mean.

4. Concluding Discussion

[36] This investigation of relationships between Antarctic cyclone characteristics and surface properties revealed many statistically significant relationships of which some can be assumed to be causal according to known physical relationships. The analysis demonstrated that the cyclone properties (I, D and R) are strongly correlated. This was to be expected, because D is related to both R and I. Large, deep systems had high precipitation, which is typical for frontal systems. The occurrence of smaller systems was concentrated over the sea ice region, where conditions were favorable for mesoscale cyclone development. Further, these results demonstrate the state-of-the-art ability of the MU tracking scheme in correctly identifying mesoscale features, creating a promising environment for future research when increasingly high-resolution pressure data will become available.

[37] Among the geographical, meteorological and surface variables, WS, IC, LE and H, P, T_s, $\partial_s T_s$, and C often had significant correlations with the cyclone properties. Many of them can be reasonably assumed to have causal relationships. The effects of latitude and season were smaller than expected, and T_s and IC, which in turn depend strongly on latitude, may 'cover' the relationships with latitude and month. On the other hand, physical circumstances impacting cyclones and the ocean surface are defined by variables as temperature and wind rather than latitude and month. Strong winds increased turbulent fluxes and the wind field modified the sea ice cover as convergent winds increased IC, while the average sea ice motion was divergent. Since the wind was related to I and D, also these variables were related to surface conditions.

[38] A challenge in explaining the factors controlling the variability of cyclonicity is that different factors are important at different temporal and spatial scales. Changes in the AMPS model configuration can also give rise to apparent interannual variability, but it is reasonable to assume that at any particular time the fundamental physical processes of surface-cyclone interaction are simulated with reasonable accuracy. Future work will involve similar work based on the ERA Interim reanalysis product, where the interannual variability can be more easily addressed, because of the temporally consistent modeling system and longer simulation periods (1989–2010).

[39] Relationships between cyclone characteristics and surface properties over the Southern Ocean and the coastal areas of Antarctica were derived for cyclones whose characteristics significantly correlated with surface properties. This has not been done before. At least 32% and possibly up to 52% of the cyclones simulated by AMPS correlated with the surface latent heat flux, sensible heat flux or temperature gradient. Approximately a quarter of these systems were mesoscale cyclones, which were generated and altered by the surface heat exchange and thermal gradients. Synoptic-scale cyclones, on the other hand, modified the underlying surface, including the sea ice cover, and were predominantly associated with baroclinicity and advection, and the atmospheric boundary layer had a little influence. For mesoscale cyclones, conversely, the boundary layer provided energy coming from instability associated with strong turbulent fluxes. Perhaps surprisingly, the impact of surface properties on mesoscale cyclones was almost as ubiquitous as the impact of synoptic-scale cyclones on surface properties, particularly in terms of temperature gradient and turbulent heat fluxes.

[40] **Acknowledgments.** We thank reviewers for their insightful comments that substantially improved the manuscript. The research was funded by the Australia Research Council grant DP0770651 and by the Academy of Finland grants 128533 and 128799. The Monash e-research facility is acknowledged for their computational support.

References

Arbetter, T. E., A. H. Lynch, and D. A. Bailey (2004), Relationship between synoptic forcing and polynya formation in the Cosmonaut Sea: 1. Polynya climatology, *J. Geophys. Res.*, *109*, C04022, doi:10.1029/2003JC001837.

Bromwich, D. H. (1991), Mesoscale cyclogenesis over the southwestern Ross Sea linked to strong katabatic winds, *Mon. Weather Rev.*, *119*, 1736–1752, doi:10.1175/1520-0493(1991)119<1736:MCOTSR>2.0.CO;2.

Bromwich, D. H., F. M. Robasky, R. I. Cullather, and M. L. Van Woert (1995), The atmospheric hydrologic cycle over the Southern Ocean and Antarctica from operational numerical analyses, *Mon. Weather Rev.*, *123*, 3518–3538, doi:10.1175/1520-0493(1995)123<3518:TAHCOT>2.0.CO;2.

Bromwich, D. H., J. J. Cassano, T. Klein, G. Heinemann, K. M. Hines, K. Steffen, and J. E. Box (2001), Mesoscale modeling of katabatic winds over Greenland with the Polar MM5, *Mon. Weather Rev.*, *129*, 2290–2309, doi:10.1175/1520-0493(2001)129<2290:MMOKWO>2.0.CO;2.

Bromwich, D. H., A. J. Monaghan, J. G. Powers, J. J. Cassano, H.-L. Wei, Y.-H. Kuo, and A. Pellegrini (2003), Antarctic Mesoscale Prediction System (AMPS): A case study from the 2000–01 field season, *Mon. Weather Rev.*, *131*, 412–434, doi:10.1175/1520-0493(2003)131<0412:AMPSAA>2.0.CO;2.

Bromwich, D. H., A. J. Monaghan, K. W. Manning, and J. G. Powers (2005), Real-time forecasting for the Antarctic: An evaluation of the Antarctic Mesoscale Prediction System (AMPS), *Mon. Weather Rev.*, *133*, 579–603, doi:10.1175/MWR-2881.1.

Bromwich, D. H., R. L. Fogt, K. I. Hodges, and J. E. Walsh (2007), A tropospheric assessment of the ERA-40, NCEP, and JRA-25 global reanalyses in the polar regions, *J. Geophys. Res.*, *112*, D10111, doi:10.1029/2006JD007859.

Carleton, A. M., and D. A. Carpenter (1990), Satellite climatology of 'polar lows' and broad-scale climatic associations for the Southern Hemisphere, *Int. J. Climatol.*, *10*, 219–246, doi:10.1002/joc.3370100302.

Carleton, A. M., and M. Fitch (1993), Synoptic aspects of Antarctic mesocyclones, *J. Geophys. Res.*, *98*, 12,997–13,018, doi:10.1029/92JD02132.

Carrasco, J. F., and D. H. Bromwich (1993), Mesoscale cyclogenesis dynamics over the southwestern Ross Sea, Antarctica, *J. Geophys. Res.*, *98*, 12,973–12,995, doi:10.1029/92JD02821.

Carrasco, J. F., D. H. Bromwich, and A. J. Monaghan (2003), Distribution and characteristics of mesoscale cyclones in the Antarctic: Ross Sea eastward to the Weddell Sea, *Mon. Weather Rev.*, *131*, 289–301, doi:10.1175/1520-0493(2003)131<0289:DACOMC>2.0.CO;2.

Cassano, J. J., J. E. Box, D. H. Bromwich, L. Li, and K. Steffen (2001), Evaluation of polar MM5 simulations of Greenland's atmospheric circulation, *J. Geophys. Res.*, *106*, 33,867–33,889, doi:10.1029/2001JD900044.

Claud, C., A. M. Carleton, B. Duchiron, and P. Terray (2009a), Atmospheric and upper ocean environments of Southern Ocean polar mesocyclones in the transition season months and associations with teleconnections, *J. Geophys. Res.*, *114*, D23104, doi:10.1029/2009JD011995.

Claud, C., A. M. Carleton, B. Duchiron, and P. Terray (2009b), Southern Hemisphere winter cold-air mesocyclones: Climatic environments and associations with teleconnections, *Clim. Dyn.*, *33*, 383–408, doi:10.1007/s00382-008-0468-5.

Comiso, J. (1999), Bootstrap sea ice concentrations from NIMBUS-7 SMMR and DMSP SSM/I, 01 January 2001–31 December 2007, updated 2008, http://nsidc.org/data/nsidc-0079.html, Natl. Snow and Ice Data Cent., Boulder, Colo.

Condron, A., G. R. Bigg, and I. A. Renfrew (2006), Polar mesoscale cyclones in the northeast Atlantic: Comparing climatologies from ERA-40 and satellite imagery, *Mon. Weather Rev.*, *134*, 1518–1533, doi:10.1175/MWR3136.1.

Cullather, R. I., D. H. Bromwich, and M. L. van Woert (1998), Spatial and temporal variability of Antarctic precipitation from atmospheric methods, *J. Clim.*, *11*, 334–367, doi:10.1175/1520-0442(1998)011<0334:SATVOA>2.0.CO;2.

Delworth, T. L., and F. Zeng (2008), Simulated impact of altered Southern Hemisphere winds on the Atlantic Meridional Overturning Circulation, *Geophys. Res. Lett.*, *35*, L20708, doi:10.1029/2008GL035166.

Fantini, M., and A. Buzzi (1993), Numerical experiments on a possible mechanism of cyclogenesis in the Antarctic region, *Tellus, Ser. A*, *45*, 99–113.

Fitch, M., and A. M. Carleton (1991), Antarctic mesocyclone regimes from satellite and conventional data, *Tellus, Ser. A*, *44*, 180–196.

Genthon, C., G. Krinner, and M. Sacchettini (2003), Interannual Antarctic tropospheric circulation and precipitation variability, *Clim. Dyn.*, *21*, 289–307, doi:10.1007/s00382-003-0329-1.

Gill, A. (1982), *Atmosphere-Ocean Dynamics*, *Int. Geophys. Ser.*, vol. 30, 662 pp., Academic, San Diego, Calif.

Godfred-Spenning, C. R., and I. Simmonds (1996), An analysis of Antarctic sea-ice and extratropical cyclone associations, *Int. J. Climatol.*, *16*, 1315–1332, doi:10.1002/(SICI)1097-0088(199612)16:12<1315::AID-JOC92>3.0.CO;2-M.

Guo, Z., D. H. Bromwich, and J. J. Cassano (2003), Evaluation of Polar MM5 simulations of Antarctic atmospheric circulation, *Mon. Weather Rev.*, *131*, 384–411, doi:10.1175/1520-0493(2003)131<0384:EOPMSO>2.0.CO;2.

Heinemann, G. (1990), Mesoscale vortices in the Weddell Sea region (Antarctica), *Mon. Weather Rev.*, *118*, 779–793, doi:10.1175/1520-0493(1990)118<0779:MVITWS>2.0.CO;2.

Hines, K. M., and D. H. Bromwich (2008), Development and testing of polar WRF. Part I. Greenland ice sheet meteorology, *Mon. Weather Rev.*, *136*, 1971–1989, doi:10.1175/2007MWR2112.1.

Hodges, K. I., B. J. Hoskins, J. Boyle, and C. Thorncroft (2003), A comparison of recent reanalysis datasets using objective feature tracking: storm tracks and tropical easterly waves, *Mon. Weather Rev.*, *131*, 2012–2037, doi:10.1175/1520-0493(2003)131<2012:ACORRD>2.0.CO;2.

Hoskins, B. J., and K. I. Hodges (2005), A new perspective on Southern Hemisphere storm tracks, *J. Clim.*, *18*, 4108–4129, doi:10.1175/JCLI3570.1.

Irving, D., I. Simmonds, and K. Keay (2010), Mesoscale cyclone activity over the ice-free Southern Ocean: 1999–2008, *J. Clim.*, *23*, 5404–5420, doi:10.1175/2010JCLI3628.1.

King, J. C., and J. Turner (1997), *Antarctic Meteorology and Climatology*, 409 pp., Cambridge Univ. Press, Cambridge, U. K., doi:10.1017/CBO9780511524967.

Krinner, G., O. Magand, I. Simmonds, C. Genthon, and J.-L. Dufresne (2007), Simulated Antarctic precipitation and surface mass balance at the end of the twentieth and twenty-first centuries, *Clim. Dyn.*, *28*, 215–230, doi:10.1007/s00382-006-0177-x.

Lim, E.-P., and I. Simmonds (2002), Explosive cyclone development in the Southern Hemisphere and a comparison with Northern Hemisphere events, *Mon. Weather Rev.*, *130*, 2188–2209, doi:10.1175/1520-0493(2002)130<2188:ECDITS>2.0.CO;2.

Lim, E.-P., and I. Simmonds (2007), Southern Hemisphere winter extratropical cyclone characteristics and vertical organization observed with the ERA-40 reanalysis data in 1979–2001, *J. Clim.*, *20*, 2675–2690, doi:10.1175/JCLI4135.1.

Lubin, D., R. A. Wittenmyer, D. H. Bromwich, and G. J. Marshall (2008), Antarctic Peninsula mesoscale cyclone variability and climatic impacts influenced by the SAM, *Geophys. Res. Lett.*, *35*, L02808, doi:10.1029/2007GL032170.

Lynch, A. H., P. Uotila, and J. J. Cassano (2006), Changes in synoptic weather patterns in the polar regions in the 20th and 21st centuries. Part 2: Antarctic, *Int. J. Climatol.*, *26*, 1181–1199, doi:10.1002/joc.1305.

Mo, K. C. (2000), Relationships between low-frequency variability in the Southern Hemisphere and sea surface temperature anomalies, *J. Clim.*, *13*, 3599–3610, doi:10.1175/1520-0442(2000)013<3599:RBLFVI>2.0.CO;2.

Monaghan, A. J., D. H. Bromwich, W. Chapman, and J. C. Comiso (2008), Recent variability and trends of Antarctic near surface temperature, *J. Geophys. Res.*, *113*, D04105, doi:10.1029/2007JD009094.

Murray, R. J., and I. Simmonds (1991a), A numerical scheme for tracking cyclone centres from digital data. Part I: Development and operation of the scheme, *Aust. Meteorol. Mag.*, *39*, 155–166.

Murray, R. J., and I. Simmonds (1991b), A numerical scheme for tracking cyclone centres from digital data. Part II: Application to January and July general circulation model simulations, *Aust. Meteorol. Mag.*, *39*, 167–180.

Noone, D., and I. Simmonds (2002), Annular variations in moisture transport mechanisms and the abundance of δ^{18}O in Antarctic snow, *J. Geophys. Res.*, *107*(D42), 4742, doi:10.1029/2002JD002262.

Noone, D., and I. Simmonds (2004), Sea ice control of water isotope transport to Antarctica and implications for ice core interpretation, *J. Geophys. Res.*, *109*, D07105, doi:10.1029/2003JD004228.

Parish, T. R., J. J. Cassano, and M. W. Seefeldt (2006), Characteristics of the Ross Ice Shelf air stream as depicted in Antarctic Mesoscale Prediction System simulations, *J. Geophys. Res.*, *111*, D12109, doi:10.1029/2005JD006185.

Patoux, J., X. Yuan, and C. Li (2009), Satellite-based midlatitude cyclone statistics over the Southern Ocean: 1. Scatterometer-derived pressure fields and storm tracking, *J. Geophys. Res.*, *114*, D04105, doi:10.1029/2008JD010873.

Peixoto, J. P., and A. H. Oort (1992), *Physics of Climate*, 520 pp., Springer, New York.

Pezza, A. B., and T. Ambrizzi (2003), Variability of Southern Hemisphere cyclone and anticyclone behavior: Further analysis, *J. Clim.*, *16*, 1075–1083, doi:10.1175/1520-0442(2003)016<1075:VOSHCA>2.0.CO;2.

Pezza, A. B., T. Durrant, and I. Simmonds (2008), Southern Hemisphere synoptic behavior in extreme phases of SAM, ENSO, sea ice extent, and Southern Australia rainfall, *J. Clim.*, *21*, 5566–5584, doi:10.1175/2008JCLI2128.1.

Powers, J. G., A. J. Monaghan, A. M. Cayette, D. H. Bromwich, Y.-H. Kuo, and K. W. Manning (2003), Real-time mesoscale modeling over Antarctica: The Antarctic Mesoscale Prediction System, *Bull. Am. Meteorol. Soc.*, *84*, 1533–1545, doi:10.1175/BAMS-84-11-1533.

Raphael, M. N. (2003), Impact of observed sea-ice concentration on the Southern Hemisphere extratropical atmospheric circulation in summer, *J. Geophys. Res.*, *108*(D22), 4687, doi:10.1029/2002JD003308.

Rasmussen, E. A., and J. Turner (Eds.) (2003), *Polar Lows: Mesoscale Weather Systems in the Polar Regions*, 612 pp., Cambridge Univ. Press, doi:10.1017/CBO9780511524974.

Saetra, O., T. Linders, and J. B. Debernard (2008), Can polar lows lead to a warming of the ocean surface?, *Tellus, Ser. A*, *60*, 141–153.

Schlosser, E., M. G. Duda, J. G. Powers, and K. W. Manning (2008), Precipitation regime of Dronning Maud Land, Antarctica, derived from Antarctic Mesoscale Prediction System (AMPS) archive data, *J. Geophys. Res.*, *113*, D24108, doi:10.1029/2008JD009968.

Seefeldt, M. W., and J. J. Cassano (2008), An analysis of low-level jets in the greater Ross Ice Shelf region based on numerical simulations, *Mon. Weather Rev.*, *136*, 4188–4205, doi:10.1175/2008MWR2455.1.

Simmonds, I. (2003), Modes of atmospheric variability over the Southern Ocean, *J. Geophys. Res.*, *108*(C4), 8078, doi:10.1029/2000JC000542.

Simmonds, I., and W. F. Budd (1991), Sensitivity of the Southern Hemisphere circulation to leads in the Antarctic pack ice, *Q. J. R. Meteorol. Soc.*, *117*, 1003–1024, doi:10.1256/smsqj.50106.

Simmonds, I., and D. A. Jones (1998), The mean structure and temporal variability of the semiannual oscillation in the southern extratropics, *Int. J. Climatol.*, *18*, 473–504, doi:10.1002/(SICI)1097-0088(199804)18:5<473::AID-JOC266>3.0.CO;2-0.

Simmonds, I., and K. Keay (2000), Mean Southern Hemisphere extratropical cyclone behavior in the 40-year NCEP-NCAR reanalysis, *J. Clim.*, *13*, 873–885, doi:10.1175/1520-0442(2000)013<0873:MSHECB>2.0.CO;2.

Simmonds, I., and K. Keay (2009), Extraordinary September Arctic sea ice reductions and their relationships with storm behavior over 1979–2008, *Geophys. Res. Lett.*, *36*, L19715, doi:10.1029/2009GL039810.

Simmonds, I., and R. J. Murray (1999), Southern extratropical cyclone behavior in ECMWF analyses during the FROST Special Observing Periods, *Weather Forecast.*, *14*, 878–891, doi:10.1175/1520-0434(1999)014<0878:SECBIE>2.0.CO;2.

Simmonds, I., and X. Wu (1993), Cyclone behavior response to changes in winter Southern Hemisphere sea-ice concentration, *Q. J. R. Meteorol. Soc.*, *119*, 1121–1148, doi:10.1002/qj.49711951313.

Simmonds, I., D. A. Jones, and D. J. Walland (1998), Multi-decadal climate variability in the Antarctic region and global change, *Ann. Glaciol.*, *27*, 617–622.

Simmonds, I., R. J. Murray, and R. M. Leighton (1999), A refinement cyclone tracking methods with data from FROST, *Aust. Meteorol. Mag.*, *June*, 3549.

Simmonds, I., K. Keay, and E.-P. Lim (2003), Synoptic activity in the seas around Antarctica, *Mon. Weather Rev.*, *131*, 272–288, doi:10.1175/1520-0493(2003)131<0272:SAITSA>2.0.CO;2.

Simmonds, I., A. Rafter, T. Cowan, A. B. Watkins, and K. Keay (2005), Large-scale vertical momentum, kinetic energy and moisture fluxes in the Antarctic sea-ice region, *Boundary Layer Meteorol.*, *117*, 149–177, doi:10.1007/s10546-004-5939-6.

Skamarock, W. C., J. B. Klemp, J. Dudhia, D. O. Gill, D. M. Barker, W. Wang, and J. G. Powers (2005), A description of the advanced research WRF version 2, *NCAR/TN-468+STR*, 88 pp., Natl. Cent. for Atmos. Res., Boulder, Colo.

Skamarock, W. C., J. B. Klemp, J. Dudhia, D. O. Gill, D. M. Barker, M. G. Duda, X.-Y. Huang, W. Wang, and J. G. Powers (2008), A description of the advanced research WRF version 3, *NCAR/TN-475+STR*, 112 pp., Natl. Cent. for Atmos. Res., Boulder, Colo.

Steinhoff, D. F., D. H. Bromwich, M. Lambertson, S. L. Knuth, and M. A. Lazzara (2008), A dynamical investigation of the May 2004 McMurdo Antarctica severe wind event using AMPS, *Mon. Weather Rev.*, *136*, 7–26, doi:10.1175/2007MWR1999.1.

Tietäväinen, H., and T. Vihma (2008), Atmospheric moisture budget over Antarctica and the Southern Ocean based on the ERA-40 reanalysis, *Int. J. Climatol.*, *28*, 1977–1995, doi:10.1002/joc.1684.

Trenberth, K. E., and J. T. Fasullo (2010), Simulation of present-day and twenty-first-century energy budgets over the southern oceans, *J. Clim.*, *23*, 440–454, doi:10.1175/2009JCLI3152.1.

Turner, J., and S. Pendlebury (2004), *The International Antarctic Weather Forecasting Handbook*, 685 pp., British Antarctic Survey, Cambridge, U. K.

Turner, J., and M. Row (1989), Mesoscale vortices in the British Antarctic territory, in *Polar and Arctic Lows*, edited by P. F. Twitchell, E. A. Rasmussen, and K. L. Davidson, pp. 347–356, A. Deepak, Hampton, Va.

Turner, J., T. A. Lachlan-Cope, D. E. Warren, and C. N. Duncan (1993a), A mesoscale vortex over Halley Station, Antarctica, *Mon. Weather Rev.*, *121*, 1317–1336, doi:10.1175/1520-0493(1993)121<1317:AMVOHS>2.0.CO;2.

Turner, J., T. A. Lachlan-Cope, and J. P. Thomas (1993b), A comparison of Arctic and Antarctic Mesoscale vortices, *J. Geophys. Res.*, *98*, 13,019–13,034, doi:10.1029/92JD02426.

Turner, J., J. C. Comiso, G. J. Marshall, T. A. Lachlan-Cope, T. Bracegirdle, T. Maksym, M. P. Meredith, Z. Wang, and A. Orr (2009a), Non-annular atmospheric circulation change induced by stratospheric ozone depletion and its role in the recent increase of Antarctic sea ice extent, *Geophys. Res. Lett.*, *36*, L08502, doi:10.1029/2009GL037524.

Turner, J., S. N. Chenoli, A. abu Samah, G. Marshall, T. Phillips, and A. Orr (2009b), Strong wind events in the Antarctic, *J. Geophys. Res.*, *114*, D18103, doi:10.1029/2008JD011642.

Udagawa, Y., Y. Tachibana, and K. Yamazaki (2009), Modulation in interannual sea ice pattern in the Southern Ocean in association with large-scale atmospheric mode shift, *J. Geophys. Res.*, *114*, D21103, doi:10.1029/2009JD011807.

Ulbrich, U., G. C. Leckebusch, and J. G. Pinto (2009), Extra-tropical cyclones in the present and future climate: A review, *Theor. Appl. Climatol.*, *96*, 117–131, doi:10.1007/s00704-008-0083-8.

Uotila, J. P., T. Vihma, and J. Launiainen (2000), Response of the Weddell Sea pack ice to wind forcing, *J. Geophys. Res.*, *105*, 1135–1151, doi:10.1029/1999JC900265.

Uotila, P., A. H. Lynch, J. J. Cassano, and R. I. Cullather (2007), Changes in Antarctic net precipitation in the 21st century based on Intergovernmental Panel on Climate Change (IPCC) model scenarios, *J. Geophys. Res.*, *112*, D10107, doi:10.1029/2006JD007482.

Uotila, P., A. H. Lynch, A. B. Pezza, K. Keay, and J. J. Cassano (2009), A comparison of low pressure system statistics derived from a high resolution NWP output and three re-analysis products over the Southern Ocean, *J. Geophys. Res.*, *114*, D17105, doi:10.1029/2008JD011583.

Vallis, G. K. (2006), *Atmospheric and Ocean Dynamics: Fundamentals and Large-Scale Circulation*, 745 pp., Cambridge Univ. Press, Cambridge, U. K., doi:10.1017/CBO9780511790447.

van den Broeke, M. R. (1998), The semi-annual oscillation and Antarctic climate. Part 2: Recent changes, *Antarct. Sci.*, *10*, 184–191, doi:10.1017/S095410209800025X.

van Lipzig, N. P. M., and M. R. van den Broeke (2002), A model study on the relation between atmospheric boundary-layer dynamics and poleward atmospheric moisture transport in Antarctica, *Tellus, Ser. A*, *54*, 497–511.

Walsh, K. J. E., I. Simmonds, and M. Collier (2000), Sigma-coordinate calculation of topographically forced baroclinicity around Antarctica, *Dyn. Atmos. Oceans*, *33*, 1–29, doi:10.1016/S0377-0265(00)00054-3.

Wang, X. L., V. R. Swail, and F. W. Zwiers (2006), Climatology and changes of extratropical cyclone activity: Comparison of ERA-40 with NCEP-NCAR reanalysis for 1958–2001, *J. Clim.*, *19*, 3145–3166, doi:10.1175/JCLI3781.1.

Wassermann, S., C. Schmitt, C. Kottmeier, and I. Simmonds (2006), Coincident vortices in Antarctic wind fields and sea ice motion, *Geophys. Res. Lett.*, *33*, L15810, doi:10.1029/2006GL026005.

Watkins, A. B., and I. Simmonds (1995), Sensitivity of numerical prognoses to Antarctic sea ice distribution, *J. Geophys. Res.*, *100*, 22,681–22,696, doi:10.1029/95JC02581.

Yuan, X., J. Patoux, and C. Li (2009), Satellite-based midlatitude cyclone statistics over the Southern Ocean: 2. Tracks and surface fluxes, *J. Geophys. Res.*, *114*, D04106, doi:10.1029/2008JD010874.

Zou, C.-Z., M. L. van Woert, C. Xu, and K. Syed (2004), Assessment of the NCEP-DOE reanalysis-2 and TOVS Pathfinder A moisture fields and their use in Antarctic net precipitation estimates, *Mon. Weather Rev.*, *132*, 2463–2476, doi:10.1175/1520-0493(2004)132<2463:AOTNRA>2.0.CO;2.

K. Keay, A. B. Pezza, and I. Simmonds, School of Earth Sciences, University of Melbourne, Melbourne, VIC 3010, Australia.

A. H. Lynch, School of Geography and Environmental Science, Monash University, Melbourne, VIC 3800, Australia.

P. Uotila, CSIRO Marine and Atmospheric Research, Private Bag 1, Aspendale, VIC 3195, Australia. (petteri.uotila@csiro.au)

T. Vihma, Finnish Meteorological Institute, FI-00101 Helsinki, Finland.